ndt
Nephrology Dialysis Transplantation

Clinical, histopathologic and molecular features of idiopathic and diabetic nodular mesangial sclerosis in humans

Michael T. Eadon [1,†], Sam Lampe[1,†], Mirza M. Baig[1,†], Kimberly S. Collins[1], Ricardo Melo Ferreira[1], Henry Mang[1], Ying-Hua Cheng[1], Daria Barwinska[1], Tarek M. El-Achkar[1], Tae-Hwi Schwantes-An[2], Seth Winfree[1,3], Constance J. Temm[4], Michael J. Ferkowicz[1], Kenneth W. Dunn[1], Katherine J. Kelly[1], Timothy A. Sutton[1], Sharon M. Moe[1], Ranjani N. Moorthi[1], Carrie L. Phillips[4] and Pierre C. Dagher[1] for the Kidney Precision Medicine Project

[1]Department of Medicine, Indiana University School of Medicine, Indianapolis, IN, USA; [2]Department of Medical and Molecular Genetics, Indiana University School of Medicine, Indianapolis, IN, USA; [3]Department of Cellular and Integrative Physiology, Indiana University School of Medicine, Indianapolis, IN, USA and [4]Department of Pathology and Laboratory Medicine, Indiana University School of Medicine, Indianapolis, IN, USA

Correspondence to: Michael T. Eadon; E-mail: meadon@iupui.edu
[†] Equal contribution among co-first authors.

ABSTRACT

Background. Idiopathic nodular mesangial sclerosis, also called idiopathic nodular glomerulosclerosis (ING), is a rare clinical entity with an unclear pathogenesis. The hallmark of this disease is the presence of nodular mesangial sclerosis on histology without clinical evidence of diabetes mellitus or other predisposing diagnoses. To achieve insights into its pathogenesis, we queried the clinical, histopathologic and transcriptomic features of ING and nodular diabetic nephropathy (DN).

Methods. All renal biopsy reports accessioned at Indiana University Health from 2001 to 2016 were reviewed to identify 48 ING cases. Clinical and histopathologic features were compared between individuals with ING and DN ($n = 751$). Glomeruli of ING ($n = 5$), DN ($n = 18$) and reference (REF) nephrectomy ($n = 9$) samples were isolated by laser microdissection and RNA was sequenced. Immunohistochemistry of proline-rich 36 (PRR36) protein was performed.

Results. ING subjects were frequently hypertensive (95.8%) with a smoking history (66.7%). ING subjects were older, had lower proteinuria and had less hyaline arteriolosclerosis than DN subjects. Butanoate metabolism was an enriched pathway in ING samples compared with either REF or DN samples. The top differentially expressed gene, *PRR36*, had increased expression in glomeruli 248-fold [false discovery rate (FDR) $P = 5.93 \times 10^{-6}$] compared with the REF and increased 109-fold (FDR $P = 1.85 \times 10^{-6}$) compared with DN samples. Immunohistochemistry revealed a reduced proportion of cells with perinuclear reaction in ING samples as compared to DN.

Conclusions. Despite similar clinical and histopathologic characteristics in ING and DN, the uncovered transcriptomic signature suggests that ING has distinct molecular features from nodular DN. Further study is warranted to understand these relationships.

Keywords: diabetic nephropathy, laser microdissection, nodule, PRR36, transcriptomics

INTRODUCTION

Idiopathic nodular mesangial sclerosis, also called idiopathic nodular glomerulosclerosis (ING), is an uncommon form of glomerular disease associated with a poor prognosis. ING was described by Alpers and Biava in 1989 [1] as a diagnosis of exclusion, characterized by nodular mesangial matrix expansion without an alternate predisposing clinical diagnosis. ING is presently considered a distinct clinical–pathological entity with light microscopic and electron microscopic features indistinguishable from those of diabetic nodular glomerulosclerosis or nodular diabetic nephropathy (DN), but without evidence of abnormal glucose metabolism or other specific diseases [2]. The disease is uncommon, with only a handful of prior case series examining the clinical and histopathologic features. These prior studies demonstrated a close association with hypertension and smoking [3–7]. A case series of 15 patients by Li and Verani [5] also found a significantly higher than expected incidence of obesity in patients with ING. The clinical presentation of ING is similar to other glomerular diseases and is characterized by

What is already known about this subject?

- the rare nature of idiopathic nodular mesangial sclerosis, also called idiopathic nodular glomerulosclerosis (ING), has led to a knowledge gap regarding the pathophysiology of this kidney disease;
- it is difficult to distinguish ING from diabetic nephropathy (DN) by histopathology; and
- this study proceeds from broad epidemiology down to the transcriptomic signature of glomeruli, examining the clinical, histopathological and molecular characteristics of ING.

What this study adds?

- we present the largest set of cases to date ($n = 48$) and compare our cases to the existing literature. We define the incidence of ING as 0.74% over a 16-year period using a denominator of all initial renal biopsy specimens;
- we demonstrate that the clinical and histopathologic features of ING and nodular DN are similar, except where distinctions can be made; and
- we investigate the molecular signature of glomeruli in a subset of laser microdissected human specimens, identifying key pathways and genes that may differentiate ING from DN.

What impact this may have on practice or policy?

- the transcriptomic markers uncovered in this study may help to differentiate idiopathic nodular glomerular disease from DN.

renal failure and proteinuria [3–7]. Despite these associations, the pathophysiology of ING remains uncharacterized. Proposed mechanisms have included elevated advanced glycosylation end products [8], increased insulin resistance in the absence of clinical diabetes [6], free radical oxidative stress from cigarette smoke [9], hormonal signaling from obesity [4, 5], increased extracellular matrix production and angiogenesis [3], and hypoxia [9], although data supporting each potential mechanism are limited. Because of the paucity of information regarding this disease and lack of prospective trials, best treatment practices remain unclear.

Distinguishing ING from nodular DN may prove important. In contrast to the uncommon nature of ING, DN is the leading cause of chronic kidney disease and end-stage renal disease worldwide [10]. The pathophysiology of diabetic kidney disease is complex and includes increased intracellular glucose concentration leading to alterations in glucose metabolism, non-enzymatic glycosylation, mitochondrial dysfunction causing reactive oxygen species and metabolic derangements including elevated free fatty acids and elevated insulin [11]. A renal biopsy is not routinely performed to diagnose diabetic kidney disease because the diagnosis is often made clinically. In those diabetics who have been biopsied, pathologic derangements include glomerular basement membrane (GBM) thickening followed by mesangial expansion secondary to cellular hypertrophy and increased matrix secretion. Later stage manifestations include nodular mesangial sclerosis (Kimmelstein–Wilson nodules) and finally global glomerular sclerosis. Extra-glomerular findings also include hyaline arteriolosclerosis, interstitial fibrosis and tubular atrophy (IFTA) [12]. Although nodular glomerulosclerosis is a pathologic feature of diabetic kidney disease, it is

not exclusive to the disease. The differential diagnosis for nodular glomerulosclerosis is extensive and may occur in the setting of membranoproliferative glomerulopathy, amyloidosis, monoclonal immunoglobulin deposition disease, fibrillary and immunotactoid glomerulopathy [6]. A diagnosis of ING is made only when these other etiologies have been excluded by history, laboratory data and a nephropathologist's examination of the renal biopsy specimen by light, immunofluorescent and electron microscopy.

We hypothesized that glomeruli of ING subjects would hold a distinct molecular signature from that of nodular DN, despite similar clinical and histopathologic characteristics, in subjects who underwent a renal biopsy in the Biopsy Biobank Cohort of Indiana (BBCI) [13]. Transcriptomic signatures of ING specimens were compared with the signatures of glomeruli obtained from nodular DN specimens and reference (REF) nephrectomies from the Kidney Precision Medicine Project (KPMP; http://www.KPMP.org). This investigation contributes to our understanding of the underlying risk factors, presentation and molecular features of ING with the goal of elucidating the pathogenesis and improving diagnostic options.

MATERIALS AND METHODS

Patient population

This study is a retrospective review of the BBCI [13]. All initial native renal biopsy specimens ($n = 6455$) acquired in standard clinical practice and processed at the Renal Pathology Laboratory at Indiana University Health Pathology Laboratory from January 2001 to December 2016 were reviewed for the presence of nodular glomerulosclerosis by natural language

processing (NLP). Only initial biopsy specimens were included in the analysis, while any subsequent specimens acquired from the same subject were excluded. Manual electronic health record (EHR) chart review was used to exclude false positives from all 180 subjects suspected to have ING to confirm the absence of DN, paraprotein-related disease or other nodule-forming glomerulopathies. Subjects were excluded from the analysis if they had insufficient clinical data to rule out the presence of diabetes mellitus (DM). Cases ($n = 48$) were classified as ING if the primary or co-primary diagnosis assigned by a nephropathologist was nodular mesangial sclerosis in the absence of DM, paraprotein disease or another glomerular disease such as primary focal segmental glomerulosclerosis (FSGS), membranoproliferative glomerulonephritis and fibrillary or immunotactoid disease. DM was defined by the presence of any of the following at any time prior or up to 6 months after the biopsy date: (i) any clinical documentation of DM in the EHR; (ii) any hemoglobin A1C $\geq 6.5\%$; (iii) any fasting blood glucose $\geq 126\,mg/dL$; (iv) any two random glucose $\geq 200\,mg/dL$ on two separate days; and (v) prior use of any antidiabetic medication other than transient sliding scale insulin. Paraprotein disease was defined by any clinical documentation of a paraprotein or the presence of a monoclonal protein on any prior serum or urine protein electrophoresis. This study was approved by the Institutional Review Board at the Indiana University School of Medicine, Indianapolis IN (#1906572234).

Clinical and pathology measurements

Demographics, clinical characteristics, laboratory values and pathology measurements were obtained from five major hospital systems within the Indiana Network for Patient Care as previously described [13]. Nodular glomerulosclerosis was defined by the presence of one or more glomeruli with nodular expansion of the mesangial matrix by light or electron microscopy [14, 15]. Severity of both ING and DN specimens was classified according to the 2010 Renal Pathology Society (RPS) guidelines [12, 16]. Briefly, specimens were classified as follows: Class II—nodular mesangial matrix expansion, with either nodular accentuation on light microscopy or nodular expansion by electron microscopy; Class III—at least one convincing round or oval nodular lesion with an acellular hyaline core; Class IV—Class II or III with >50% global glomerulosclerosis. Although qualifying as Class II by RPS guidelines, specimens with mesangial matrix expansion without nodular features were excluded from the study. Glomerular obsolescence, hyaline arteriolosclerosis and IFTA were categorized as none ($\leq 10\%$ of affected glomeruli or kidney parenchyma), mild (11–30%), moderate (31–60%) or severe (>60% affected). One nephropathologist (C.L.P.) was responsible for interpreting 95.5% of all specimens. Acute tubular necrosis (ATN) and secondary FSGS were reported as bi-level variables according to their presence or absence. Podocyte effacement was extracted from the pathology report and ultrastructurally categorized as widespread (>75% effacement) or not widespread. GBM thickness was extracted from the pathology report for all available samples.

The renal pathologist reviewed 47 ING and 10 DN periodic acid–Schiff stained sections to quantify extra efferent arterioles.

Sections at multiple levels were reviewed to identify the vascular pole of every glomerulus (if possible) and the total quantity of arterioles was recorded for each glomerulus with a visible vascular pole. Neoarterioles were not counted in obsolescent glomeruli or twin glomeruli with shared vessels. Neoarterioles were counted outside of Bowman's capsule at vascular pole.

Laser capture and RNA isolation

A total of 32 specimens from three groups underwent glomerular laser microdissection. Group #1 consisted of 5 of the 48 ING specimens that had sufficient frozen tissue remaining in their optimal cutting temperature (OCT) compound block to perform laser capture of glomeruli. Group #2 included 18 specimens showing nodular DN specimens. Group #3 included nine REF samples obtained from three deceased donor nephrectomies or the unaffected cortical edge of six tumor nephrectomies (these six were obtained from the KPMP). The dissections were based on whole glomerular dissections (not nodular lesions), including all cellular glomeruli in three 10-μm cross-sections of the frozen biopsy specimen. The entire laser capture and RNA isolation protocols have been published previously [17].

RNA sequencing

After evaluation of RNA quantity and quality by an Agilent Bioanalyzer 2100 Eukaryote Total RNA Pico Chip, a minimum of one nanogram was used to construct each sample's cDNA library with the Takara SMARTer Stranded Total RNA-Seq pico input version 2 without fragmentation (Clontech, No. 634938). This platform is optimized for the sequencing of archived biosamples [18–20]. All samples met a minimum DV200 (percent of nucleotides >200 in length) standard of 25%. Prior to cDNA synthesis, rRNA was removed with the RiboGone mammalian kit protocol (Clontech, No. 634847). An Agilent Bioanalyzer was used to quantify each cDNA library and assess for adequate quality. These libraries were pooled in equal molarity of 100 pM and 8 μL from each library was added to each lane of an Illumina HiSeq 4000. An average of 100 million reads was obtained per sample.

Mapping and expression

Samples were first pre-processed to remove Smart CDS sequences and three nucleotides from each reading end. Using STAR version 2.4.2 [21], the results were then aligned and mapped to the human reference genome (hg38). Quantification of gene expression levels was obtained from FeatureCounts (subread version 1.5.0) [22] applying parameters '–Q 10'. The edgeR program was then used to assess differential expression [23]. Read counts were quantile normalized across all 32 samples. Overall, 25 550 genes were expressed in at least one sample and included in the analysis. A heatmap with dendrogram and principal component analysis (PCA) clustered samples by expression signatures. A negative binomial dispersion estimation exact test was used to determine differential expression of the genes [24]. Adjusted P-values were calculated with a Benjamini–Hochberg false discovery rate (FDR) correction.
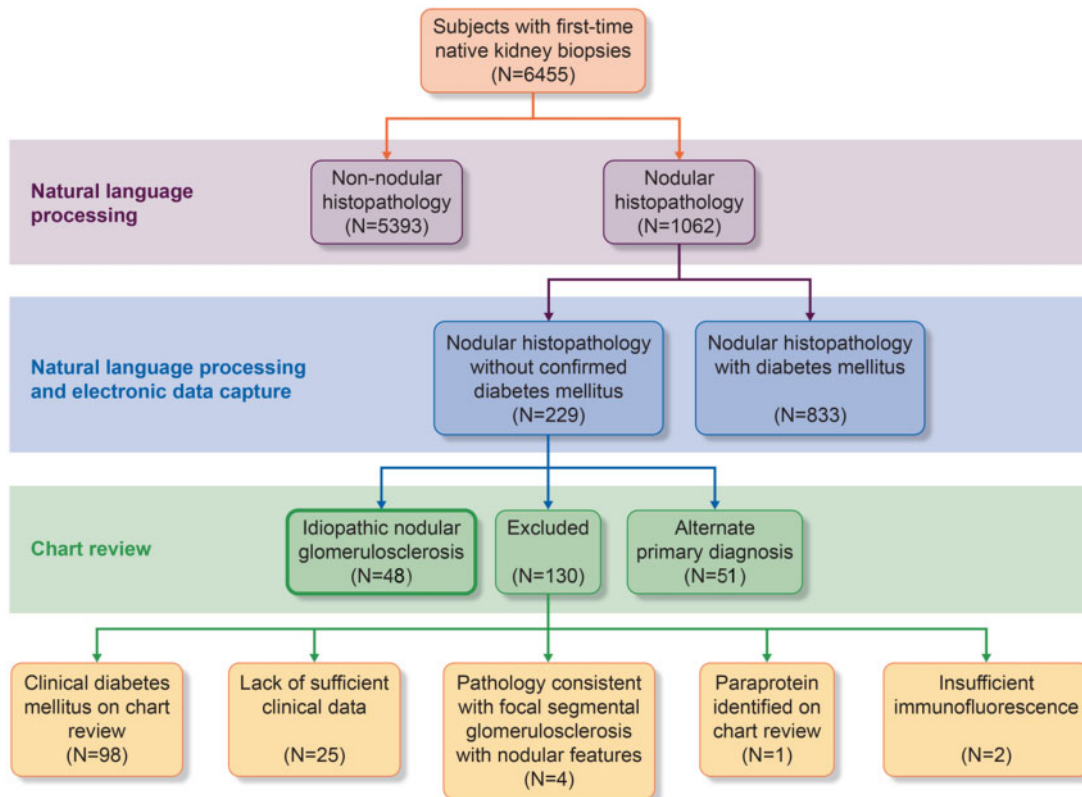
FIGURE 1: Selection process for determining members of the ING cohort. Using NLP of all biopsy reports, a total of 1062 unique individuals had a first native renal biopsy with a 'nodule', 'nodularity', 'nodular mesangial sclerosis' or other 'nodular' features. Electronic data capture identified 833 subjects as having DM. A manual chart review of the remaining 229 cases excluded individuals with evident DM on chart review, lack of sufficient data to exclude DM, inconsistent pathology, a paraprotein or insufficient immunofluorescence. Forty-eight cases were consistent with a diagnosis of ING.

Pathway analysis and transcriptogram

Genes were filtered for a pathway enrichment analysis with the Benjamini–Hochberg FDR adjusted P < 0.05 to be included in the pathway analysis. Enrichment of Gene Ontology (GO) Terms, Kyoto encyclopedia of genes and genomes (KEGG) pathways and Reactome pathways [25, 26] were tested with ReactomePA [27] or clusterProfiler [28] with a Fisher's exact test. Enrichment was considered present with an FDR <0.2. A transcriptogram was created using a transcriptogram network enrichment analysis as previously described [29]. In brief, a transcriptogram is a visual depiction of pathway enrichment wherein genes are ordered along the x-axis using a Monte Carlo Simulation that weights their gene–gene interactions. Genes belonging to similar GO, KEGG and Reactome pathways were ordered in closer proximity to each other on the x-axis according to string database interactions. The gene expression profiles from the samples are then projected onto this gene list.

Immunohistochemistry

A polyclonal antibody to proline rich 36 (PRR36; Sigma HPA062741 at 1:200 dilution; Sigma-Aldrich Corp., St Louis, MO, USA), using high pH with antigen retrieval in a Dako PT Link module, was first validated and calibrated in a human colon positive control. Paraffin-embedded 4-μm sections of ING and DN subjects were deparaffinized, subjected to antigen retrieval (20 min at 99°C) and primary antibody for 40 min. The detection was performed with a Dako Flex kit on the Link Autostainer: Rabbit linker (10 min) followed by Flex-hrp (20 min) and color development with DAB (10 min). A distinctive perinuclear reaction was observed. Two blinded observers counted total glomerular nuclei (excluding Bowman's capsule) and the proportion of cells with a perinuclear expression in at least 20 glomeruli and five samples per group. All 10 samples had <50% glomerular obsolescence. The five ING samples were the same as those laser microdissected.

Statistics

Data are reported as means ± standard error. Comparisons between clinical groups were made by two-tailed Fisher's exact test or Chi-squared test for categorical variables, t-test for continuous variables and analysis of variance (ANOVA) for continuous variables in more than two groups as appropriate.

RESULTS

Incidence of ING

Of the 6455 unique individuals who underwent a first-time native renal biopsy between 2001 and 2016 in the BBCI, 1062 were found to have nodular histopathology (Figure 1). Of these, 833 were known diabetics with 751 subjects given a primary

Table 1. Clinical characteristics

Key clinical findings	BBCI cohort	Markowitz *et al.* 2002 [3]	Li and Verani 2008 [5]	Wu *et al.* 2014 [4]	Hamrahian *et al.* 2018 [6]	Salvatore *et al.* 2015 [7]	Pooled data
N	48	23	15	20	17	4	127
Study period	2001–16	1996–2001	1998–2007	2009–11	1999–2014	2003–12	–
Mean age, years	68.1	68	64	55.5	60.2	62	64.2
Gender (M:F)	26:22	18:05	5:10	16:04	13:04	4:0	82:45
Ethnicity (White:Black:Hispanic:other)	36:6:0:6	17:6:0:0	11:3:1:0	20 Asian	7:7:1:2	4:0:0:0	75:22:2:28
Average proteinuria, g/day	4.0	4.7	5.6	2.85	3.53	3.0	4.1
Nephrotic range,[a] %	60.4	69.6	73	35	40	Unknown	56.7
Mean Cr at time of biopsy,[b] mg/dL	3.21	2.4	2.8	4.23	2.35	1.9	3.03
Renal insufficiency (Cr >1.2 mg/dL),[b] %	81.3	82.6	93	95	94	100	87.1
Hyperlipidemia, %	60.4	90	Unknown	50	Unknown	Unknown	65.3
Hypertension, %	95.8	95	93	90	100	100	95.3
Smoking, %	66.7	91	67	85	65	50	73.8
Obesity, %	42.9[c]	13	60	40	37.5[c]	Unknown	37.3

Comparison of the clinical characteristics between this study's cohort and those of prior case series including Markowitz *et al.*, Li and Verani, Wu *et al.* and Hamrahian *et al.*
[a]Normal range for proteinuria is <0.3 g/day.
[b]Normal range for serum Cr varies by age and race, but is generally ≤1.2 mg/dL. Glomerular filtration rates were not available across studies.
[c]Incomplete data are available. Data on obesity were available for 28 subjects in the BBCI cohort and 16 subjects in the Hamrahian cohort.

diagnosis of DN, 30 were considered nondiagnostic due to insufficient immunofluorescence and 52 were given an alternate primary diagnosis (e.g. glomerulonephritis) by the nephropathologist. Of the 229 subjects with nodular histopathology but no confirmed DM, 51 had an alternate primary diagnosis of glomerulonephritis, immune-mediated nephrotic syndrome, paraprotein-related kidney disease or acute kidney injury. Upon manual EHR review of the remaining 178 individuals, 130 were excluded and 48 were included in the cohort of primary ING subjects. Exclusion criteria included the presence of clinical diabetes that had not been identified by NLP or chart review of the electronic medical record ($n = 98$), the presence of a serum paraprotein without consistent biopsy specimen features ($n = 1$), insufficient clinical data to exclude DM ($n = 25$) and insufficient immunofluorescence to rule out alternate glomerular pathology ($n = 2$). Upon re-evaluation of potential ING cases by the nephropathologist, an additional four cases were excluded due to histology with dominant features of FSGS. The overall incidence of ING as a primary diagnosis was 0.74% in the BBCI cohort.

Demographics and clinical features of ING

The mean age of the ING cohort was 68.1 years old, 75% were Caucasian and 54% were male. This distribution is comparable to the overall BBCI rates of 72.7% Caucasian and 50.2% male. At the time of biopsy, 81.3% of patients had renal insufficiency [mean creatinine (Cr) of 3.21 mg/dL]. Nephrotic-range proteinuria was present in 40.5% of patients, hypertension in 95.8%, a smoking history in 66.7%, hyperlipidemia in 60.4% and obesity in 42.9%. These characteristics parallel existing ING cohorts [3–7] as depicted in Table 1.

Idiopathic nodular and nodular diabetic glomerulosclerosis

Figure 2 depicts representative images of ING and nodular DN histology and electron microscopy. The clinical and histopathologic features of the ING and nodular DN groups were compared (Table 2). The 751 individuals with a primary diagnosis of nodular DN served as comparators to the ING cohort. On balance, ING subjects were older than diabetics at the time of biopsy (68.1 versus 55.6 years, P < 0.001), had less proteinuria (4.0 versus 7.5 g/day, P < 0.001) and were more frequently smokers. Although overweight themselves, ING subjects also had lower body mass index (BMI) values (28.3 versus 31.6 kg/m², P = 0.004) compared with diabetics. Gender, race, concomitant hypertension and baseline serum Cr did not differ significantly. Regarding histology, diabetics had more frequent severe arteriolosclerosis than ING subjects (P < 0.001). Although the proportion of diabetics with thickened GBMs was higher than ING subjects (P < 0.001), the average reported thickness was not different. Glomerular obsolescence, IFTA and presence of concomitant ATN did not vary significantly. The distribution of DN severity class was similar between groups; however, ING subjects had more frequent secondary FSGS (14.6% versus 6.1%, P = 0.034). Podocyte effacement on electron microscopy was patchy or non-specific in most individuals of both groups. Cases were re-examined for neovascularization (Figure 3). ING subjects frequently had extra efferent arterioles present (65.2%). In individuals with neoarterioles, the proportion of glomeruli with neoarterioles was 36.4%, with an average total number of 7.0 arterioles (five extra) in the neovascularized glomeruli.

Transcriptomics of glomeruli in ING

To assess the underlying pathogenesis of ING, glomeruli were laser microdissected from the available ING samples. Expression was then compared with microdissected glomeruli of REF nephrectomies and nodular DN samples. A total of 25 550 genes were expressed in at least one sample. Unsupervised clustering of samples by expression of all genes was examined in a heatmap with dendrogram and PCA (Figure 4). In both methodologies, the REF samples tended to cluster most closely, albeit more clearly in the PCA. In contrast, the glomerular signatures of the ING and the nodular DN samples overlapped and were more broadly distributed.
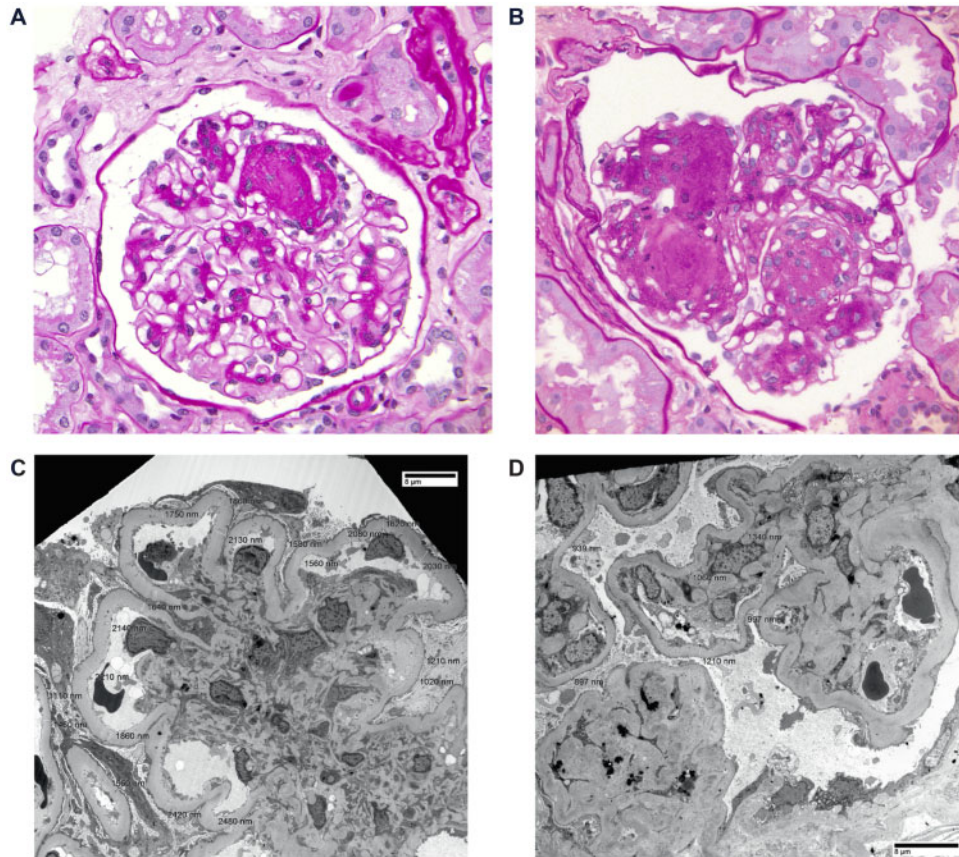
FIGURE 2: An example of ING (**A**) and diabetic glomerulosclerosis (**B**) on periodic acid–Schiff staining of paraffin-embedded sections are given. Electron microscopy images are pictured for ING (**C**) and DN (**D**).

Differentially expressed genes between idiopathic nodular and REF samples

Between the ING and REF cohort, 458 genes were differently expressed at an FDR corrected level of significance (FDR $P < 0.05$, Figure 5A, Supplementary data, Table S1). Several genes of known renal significance were differentially expressed, including *NPHS1* (nephrin), *COL4A3* and *PLCE1*. *NPHS1* expression (FDR $P = 0.008$) and expression of the basement membrane constituent *COL4A3* (FDR $P = 0.015$) were both significantly reduced in ING patients. *PLCE1*, an important mediator of podocyte formation, was also down-regulated 15.9-fold ($P = 0.0002$, FDR $= 0.02$) in ING subjects.

Table 3 depicts the top 10 differentially expressed genes (DEGs) between ING and REF samples. Among these, the most significant DEG was *PRR36*, whose expression was increased 248-fold ($P = 2.24 \times 10^{-10}$, FDR $P = 5.93 \times 10^{-6}$) compared with REF samples. *PRR36* expression was increased in four of five ING samples. *PRR36* is a protein-coding gene of unknown function [30]. The most significantly down-regulated gene was leukocyte cluster member 8 (*LENG8*), which was reduced ($\log_2$ 13.78-fold) compared with REF samples ($P = 1.15E-08$, FDR $= 0.0001$). *LENG8* is a protein-coding gene with an uncharacterized function, but has been associated with prognosis in renal cell carcinoma [31]. Neutrophil Gelatinase-Associated Lipocalin (*LCN2*) expression was significantly up-regulated (FDR $P = 0.0003$) in ING glomeruli, although this marker is classically associated with distal nephron injury.

DEGs between idiopathic nodular and diabetic samples

In an analysis of ING and nodular DN samples, 92 genes were differently expressed at an FDR $P < 0.05$ (Figure 5B and Supplementary data, Table S2). Again, the most significant DEG was *PRR36*, which was up-regulated 109-fold ($P = 6.99 \times 10^{-11}$, FDR $P = 1.85 \times 10^{-06}$) in ING samples. Two additional DEGs were down-regulated in ING samples as compared with both nodular DN and REF samples: pre-mRNA processing factor 8 (*PRPF8*) and *MLLT6*. PRPF8 is a component of the spliceosome and is implicated in retinitis pigmentosa [30]. *MLLT6* encodes the protein AF17, a transcription factor that regulates epithelial sodium channel expression. AF17 deficiency is associated with natriuresis and reduced blood pressure [32]. Expression of *LCN2*, *PLCE1*, *COL4A3* and *NPHS1* were not significantly different between ING and nodular DN. Supplementary data, Table S3 contains DEGs between DN and REF samples. Analogously to the ING samples, decreased expression of podocyte markers (NPHS1, PLCE1 and COL4A3) was observed in DN samples. *PRR36* was not differentially expressed between DN and REF samples ($\log_2$ fold change of 1.2, $P = 0.49$).

Pathway enrichment

Enrichment of GO terms, KEGG pathways and Reactome pathways was assessed in the DEGs of both ING comparisons with REF and DN samples. Figure 5C and D illustrate the most

Table 2. Histologic and clinical features

Histologic/clinical feature	ING ($n = 48$)	DN ($n = 751$)	P-value
Mean glomerular obsolescence, %	33 ± 23.7 ($n = 48$)	34.4 ± 23 ($n = 672$)	0.733
RPS classification,[a] %	$n = 48$	$n = 672$	0.15
Class II	33.3	21.9	
Class III	43.8	55.9	
Class IV	22.9	22.2	
Interstitial fibrosis/tubular atrophy, %	$n = 45$	$n = 568$	0.63
None	0	0	
Mild	11.1	8.0	
Moderate	48.9	53.5	
Severe	40.0	38.2	
Arteriolosclerosis, %	$n = 44$	$n = 601$	<0.001
None	2.3	1.5	
Mild	18.2	6.8	
Moderate	61.3	44.9	
Severe	18.2	46.8	
Extra efferent neovascularization, %	$n = 46$	$n = 10$	
Any neoarteriole present (Y)	65.2	40.0	0.29
Proportion of glomeruli with neoarterioles[b]	36.4 ± 28.1	30.7 ± 16.1	0.70
Number of arterioles present[b]	7.0 ± 4.3	4.4 ± 1.6	0.05
Podocyte effacement, %	$n = 48$	$n = 749$	0.088
Widespread or >75%	37.5	25.4	
Patchy or nonspecific	62.5	74.4	
GBM thickness	$n = 48$	$n = 601$	
GBM >520 nm in men or >471 nm in women, %	79.2	93.1	<0.001
Mean GBM thickness, nm	836 ± 322	857 ± 222	0.76
Concomitant ATN, %	18.9	15.4	0.54
Concomitant FSGS	14.6	6.1	0.034
Mean age, years	68.1 ± 13.1	55.6 ± 12.7	<0.001
Gender (M:F)	26:22	415:336	0.88
Ethnicity (White:Black:Hispanic:other)	36:6:0:6	491:173:9:78	0.33
Average proteinuria, g/day	4.0 ± 3.5 ($n = 42$)	7.5 ± 7.3 ($n = 246$)	<0.001
Nephrotic range, %	40.5 ($n = 42$)	63.4 ($n = 246$)	<0.001
Mean Cr at time of biopsy, mg/dL	3.21 ± 1.3 ($n = 46$)	3.09 ± 1.9 ($n = 415$)	0.56
Renal insufficiency (Cr >1.2 mg/dL), %	81.3 ($n = 46$)	90.1 ($n = 415$)	0.081
Hypertension, %	95.8	86.6	0.073
Smoking, %	66.7 ($n = 40$)	49.2 ($n = 415$)	0.023
Mean BMI, kg/m^2	28.3 ± 5.4 ($n = 28$)	31.6 ± 6.9 ($n = 228$)	0.004

Comparison of the histopathologic and clinical characteristics of the subjects with a primary diagnosis of ING versus subjects with a primary diagnosis of nodular DN. All available data were used, with the sample size for each group indicated when data was available for less than the entire cohort. [a]RPS guidelines for classification of DN were applied to DN and adapted for ING specimens. [b]The proportion of glomeruli with neoarterioles and total arterioles in samples with any neoarterioles, samples with no neoarterioles were excluded. The number of arterioles includes the first afferent and efferent arteriole as well as neoarterioles.

enriched pathways. A complete list is provided in Supplementary data, Tables S4 and S5. The enriched pathways of the ING–REF comparison include transcriptional regulation, DNA methylation and RUNX1 interactions. Compared with nodular DN, enrichment was found in cell signaling pathways such as interferon gamma signaling, phosphorylation of CD3 and the T-cell receptor and PD-1 signaling. *PRR36* is not a member of any KEGG or Reactome pathway, as little is known of its function.

Transcriptogram network analysis

Standard pathway enrichment tests whether the number of significant genes in a pathway exceeds the number expected by random chance. In contrast, a transcriptogram network analysis incorporates known protein–protein interactions to assess enriched pathways, level of significance, magnitude of differential expression and direction of effect. Pathway enrichment by transcriptogram network analysis for ING versus REF and ING

versus diabetic nodular glomerulosclerosis are depicted in Figure 6. Multiple pathways were enriched. Among the enriched pathways in the ING versus REF comparison, rRNA modification, meiosis, DNA replication, RAS signaling, inositol phosphate metabolism, striated muscle contraction, sphingolipid metabolism, regulation of blood pressure by the renin–angiotensin system and respiratory electron transport were enriched. Pathway comparison of the ING and diabetic nodular glomerulosclerosis groups revealed fewer enriched pathways, including homologous recombination DNA repair, response to replication stress, G protein-coupled acetylcholine receptor signaling, smell chemoreceptors, Rho GTPase cycle and isoprenoid metabolism. Butanoate metabolism was enriched in comparisons between ING and both REF and DN.

Proportion of PRR36 expressing cells is reduced

The protein expression of the top DEG, *PRR36*, was assessed in the glomeruli of the ING and nodular DN samples (Figure 7).

M.T. Eadon *et al.*

Immunohistochemistry of both ING and nodular DN samples revealed clumps of perinuclear granular PRR36 immunoperoxidase reaction of epithelial cells, including podocytes, parietal epithelial cells and proximal tubular epithelial cells. Excluding Bowman's capsule, the proportion of total glomerular nuclei with clumps of perinuclear protein expression was reduced in ING specimens as compared with diabetic specimens. In ING specimens, 31.7% of cells had perinuclear expression compared with 63.1% of diabetic specimens (P = 0.01).

DISCUSSION

ING is an uncommon form of glomerular disease. In our BBCI cohort, the overall incidence was 0.74%, which is enriched compared with other cohorts [3]. However, a smoking history (39.9% of all individuals) and peripheral vascular disease (12.4% of all individuals) were prevalent in patients who underwent a renal biopsy at our institution [13]. The ING subjects
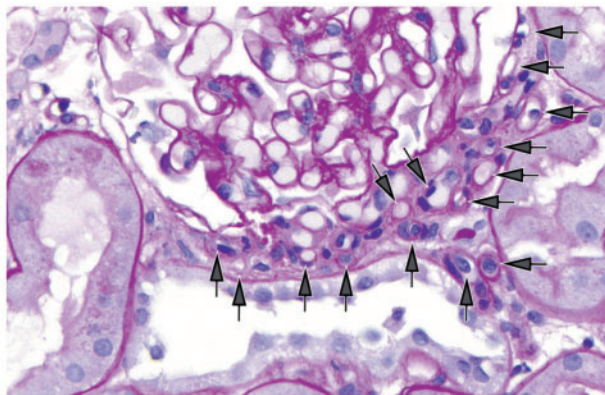

FIGURE 3: An example of neovascularization at the vascular pole of a glomerulus in a sample with nodular mesangial sclerosis. A subset of arterioles is labeled with arrows.

presented in this study were similar to prior cohorts as high rates of hypertension, proteinuria and renal failure were observed [3–6]. Regardless, the uncommon nature of this disease has led to a knowledge gap regarding the pathophysiology and treatment options for patients with ING. Currently, ING patients are managed conservatively with smoking cessation and antihypertensive therapy. This study proceeds from epidemiology down to the transcriptomic signature of glomeruli, examining the clinical, histopathological and molecular characteristics of ING. These features benefit from comparisons with individuals with nodular DN.

Most histopathologic characteristics were similar between ING and nodular DN subjects, as all included subjects had mesangial sclerosis with nodule formation. The severity of nodular disease, degree of glomerular obsolescence and interstitial fibrosis were aligned in each group. Both groups displayed neovascularization of glomeruli, as previously reported [3, 7, 33, 34]. Compared with diabetics, the ING patients had less hyaline arteriolosclerosis and proteinuria at the time of biopsy. We speculate these differences are related to sampling bias, as clinicians may be less inclined to biopsy known diabetics with less severe disease.

As expected, more DEGs were identified in the ING–REF analysis than the ING–DN comparison. The REF samples had fewer obsolescent glomeruli and lacked nodularity. In contrast, the histopathologic characteristics of the ING and DN samples were similar. Among the DEGs of ING and REF samples, upregulation of the injury marker *LCN2* was observed. Downregulation was observed for podocyte markers like *NPHS1* and *PLCE1*, which may be related to podocyte cell loss in glomeruli. *PLCE1* encodes a phospholipase enzyme that hydrolyzes phosphatidylinositol-4,5-bisphosphate to inositol 1,4,5-triphosphate (IP3) and diacylglycerol (DAG). IP3 and DAG are linked with regulation of cell growth, differentiation and podocyte formation [35]. *PLCE1* mutations have been implicated in
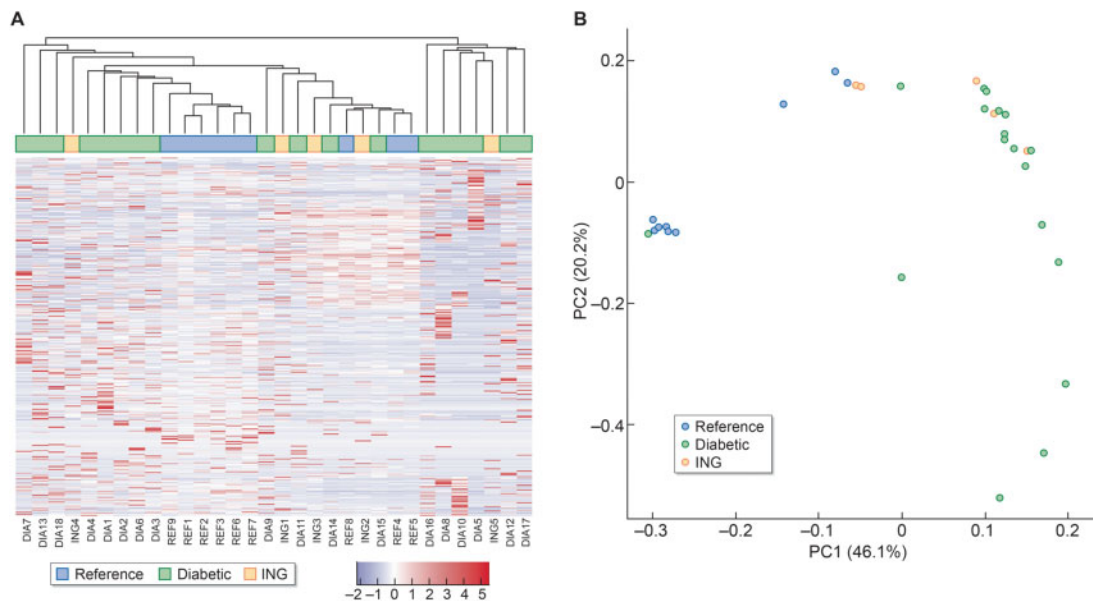

FIGURE 4: (**A**) Unsupervised heatmap including dendrogram illustrating the relative gene expression between ING, nodular DN and REF samples. (**B**) PCA plot showing gene expression clustering of the samples. The REF samples cluster more closely while the ING and nodular DN transcriptomic signatures are more broadly distributed.
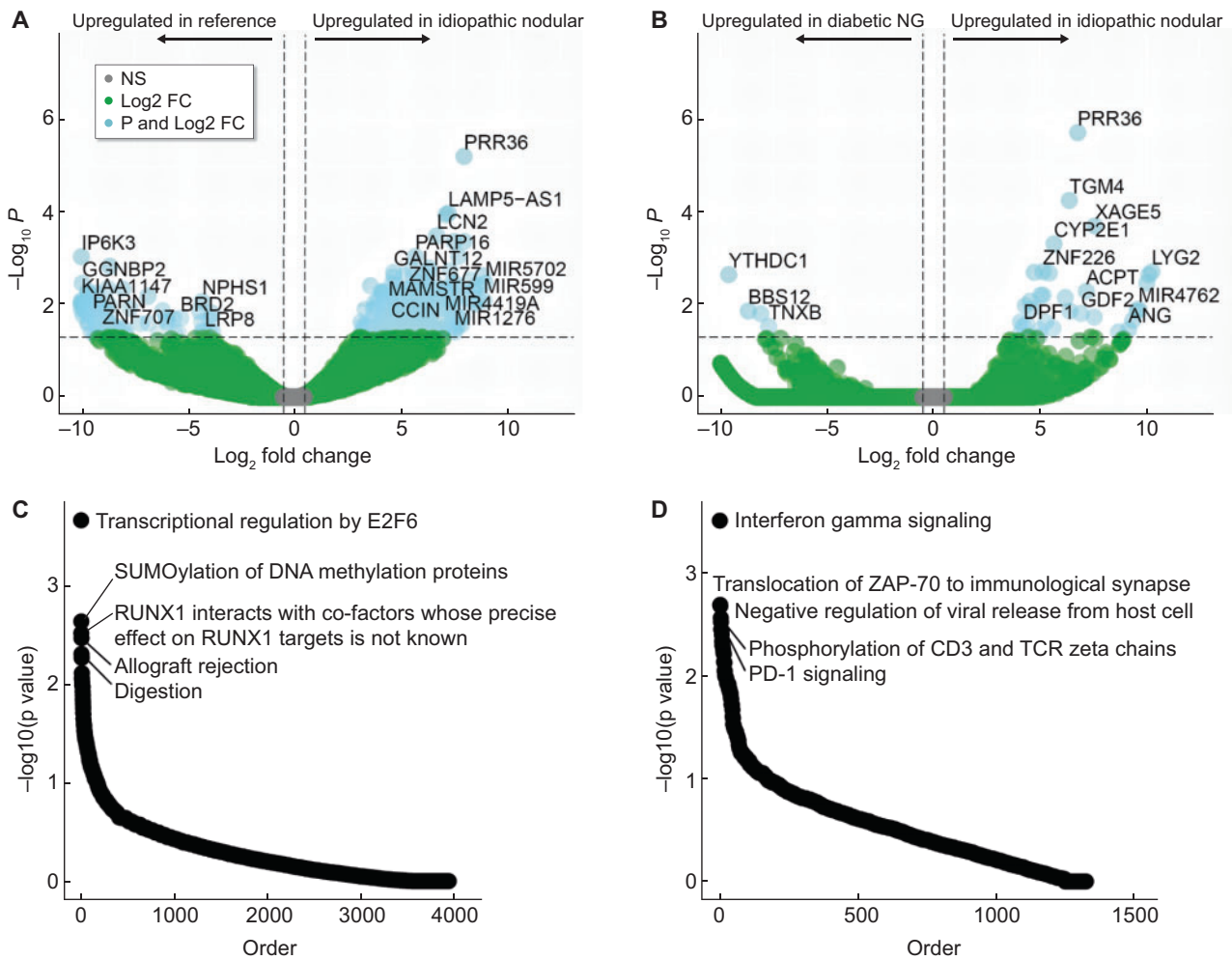
FIGURE 5: Volcano plot illustrating differentially expressed transcripts between ING and REF samples (**A**) and ING versus nodular DN (nodular glomerulosclerosis) (**B**). *PRR36* was differentially expressed in ING compared with both REF and diabetic nodular samples. Horizontal dotted lines represent FDR <0.05. Vertical dotted lines represent log$_2$ fold change (FC) >0.25. (**C**) Enriched pathways in the ING and REF analysis. (**D**) Enriched pathways in ING and diabetic analysis.

hereditary nephrotic syndrome and steroid-resistant nephrotic syndrome [36, 37]. Decreased expressions of glomerular *PLCE1* and *NPHS1* are also observed in diabetic kidney disease [38], as similarly confirmed in this study. Thus, the reduced number of DEGs in the ING–DN comparison is unsurprising.

One hypothesis is that ING is a manifestation of early hyperglycemia, on the spectrum of DN [39, 40]. Despite similar clinical and histopathologic characteristics, multiple DEGs were identified between ING and DN glomeruli. Among the differentially expressed pathways in ING and DN, the transcriptogram analysis revealed that butanoate metabolsim was enriched in comparisons between ING with both REF and nodular DN. Butyrate has been postulated as a potential therapy to reduce pro-fibrotic cytokine generation [41, 42]. The standard pathway enrichment analysis also identified immune cell signaling pathways, implicating a differential effect of the immune system in ING and nodular DN. Thus, the signatures uncovered suggest ING is a distinct pathophysiological entity from nodular DN.

Both *PRR36* transcript and protein levels were differentially expressed. *PRR36* was highly up-regulated in ING glomeruli;

however, protein expression was reduced. *PRR36* mRNA expression may be elevated in compensation for the reduced protein. Little is known of PRR36 function except that it is a protein-coding gene and has known expression in the brain [30]. While PRR36 gene or protein expression may aid in differentiating ING and nodular DN, it is unclear whether *PRR36* plays a role in pathogenesis of ING. Additional study is warranted in a larger human population and in animal models to confirm or refute this supposition.

The small sample size employed in the transcriptomic analysis is one of the limitations of our study. Of the 48 ING subjects identified in the 16-year period, only 5 had remnant samples with sufficient glomeruli found in the OCT block that yielded adequate RNA quantity and quality. A greater number of diabetic samples were available for comparison. The sample size limited our power to detect subtle differential expression of genes and increases the risk of false positives. However, this limitation is inherent when studying an uncommon disease. An additional limitation is that whole glomeruli were dissected, not nodular lesions. Indeed, the PRR36-positive cells were identified outside

M.T. Eadon *et al.*

Table 3. Top 10 most DEGs

Gene	Log$_2$ fold change	CPM	P-value	FDR	Top related pathway[b]	Pathway term
ING versus REF						
PRR36	7.95	297.3	2.24E-10	5.93E-06	None	–
LAMP5-AS1	7.21	46.3	8.23E-09	0.000101	None	–
LENG8	−13.78	254.3	1.15E-08	0.000101	None	–
NAT16	7.11	99.1	1.67E-08	0.000111	None	–
GABBR1	−11.99	74.0	3.19E-08	0.000169	Activation of G protein gated potassium channels[a]	R-HSA-1296041
LCN2	6.68	30.9	7.23E-08	0.000314	Cellular iron ion homeostasis	GO: 0006879
PRPF8	−11.95	72.1	9.46E-08	0.000314	Spliceosome[a]	hsa03040
DLG5	−12.57	110.8	1.06E-07	0.000314	Protein localization to cell junction[a]	GO: 1902414
MLLT6	−12.51	106.2	1.07E-07	0.000314	None	–
INTS3	7.48	97.9	1.30E-07	0.000344	Mitotic cell cycle checkpoint	GO: 0007093
ING versus diabetic nodular glomerulosclerosis						
PRR36	6.77	185.8	6.99E-11	1.85E-06	None	–
TGM4	6.37	87.3	4.13E-09	5.47E-05	Peptide cross-linking	GO: 0018149
XAGE5	7.58	31.1	2.21E-08	0.000195	None	–
CYP2E1	5.65	98.7	7.21E-08	0.000477	Drug metabolism—cytochrome P450	hsa00982
SNORA54	−12.85	165.1	2.13E-07	0.001131	None	–
SPRY3	−12.58	136.9	4.24E-07	0.001604	None	–
PRPF8	−12.58	136.9	4.24E-07	0.001604	mRNA splicing—major pathway[a]	R-HSA-72163
ANKRD20A9P	−12.41	121.7	6.43E-07	0.001904	None	–
MLLT6	−12.37	118.3	7.11E-07	0.001904	None	–
DHX16	−12.32	114.8	7.9E-07	0.001904	mRNA splicing—major pathway[a]	R-HSA-72163

Comparisons made to the ING cohort with both REF and nodular DN by a negative binomial dispersion estimation exact test. Fold change is positive if up-regulated in ING and negative if up-regulated in comparison. CPM stands for counts per million for gene expression. Both P-values and Benjamini–Hochberg FDR are listed for each gene. [b]Genes may contribute to multiple pathways, listed is the most significantly enriched pathway. The GO term, KEGG pathway or Reactome pathway is provided. [a]Pathway enrichment at P < 0.05.

of nodules and the transcriptomic signature may be very different in nodules than the remaining glomerulus or when using alternative platforms that better localize transcripts such as spatial transcriptomics. Finally, representation bias is present. Patients rarely undergo a renal biopsy for mild disease or when the diagnosis is known. Thus, the sample of nodular DN biopsy specimens is not representative of the greater DN population.

These limitations are counterbalanced by significant strengths. First, this is a large series of 48 ING patients culled from the BBCI renal biopsy cases ($n = 6455$). The next largest reported cohort that was identified consisted of 23 patients [3]. Second, all cases underwent strict evaluation by manual review to eliminate false-positive cases. Finally, this study marks a first step in understanding the expression signature unique to glomeruli in ING subjects, identifying distinct features from nodular DN. The insights provided into the pathogenesis of ING may help guide future diagnostic tools and aid pathologists in distinguishing ING from diabetic nodular mesangial sclerosis.

SUPPLEMENTARY DATA

Supplementary data are available at ndt online.

AUTHORS' CONTRIBUTIONS

Conception, analysis and interpretation of data was conducted by M.T.E., S.L., M.B., D.B., R.M.F., H.M., Y.-H.C., K.S.C., S.W., M.J.F. and P.C.D. Drafting/revising the article was done by M.T.E., S.L., M.B., T.M.E. and P.C.D. C.L.P., K.J.K., T.-H.S.-A., K.W.D., C.J.T., R.M.F., T.A.S. and S.S.M. provided intellectual content. All authors involved in final approval of the version to be published.

CONFLICT OF INTEREST STATEMENT

T.-H.S.-A is a paid consultant for Target Pharmasolutions. S.S.M. is a scientific advisor for Sanifit, Amgen and Ardelyz. The results presented in this article have not been published previously in whole or part, except in abstract format.

DATA AVAILABILITY STATEMENT

Data are archived in the Gene Expression Omnibus (GEO # GSE162830) and in the KPMP atlas (https://atlas.kpmp.org).

REFERENCES

1. Alpers CE, Biava CG. Idiopathic lobular glomerulonephritis (nodular mesangial sclerosis): a distinct diagnostic entity. *Clin Nephrol* 1989; 32: 68–74
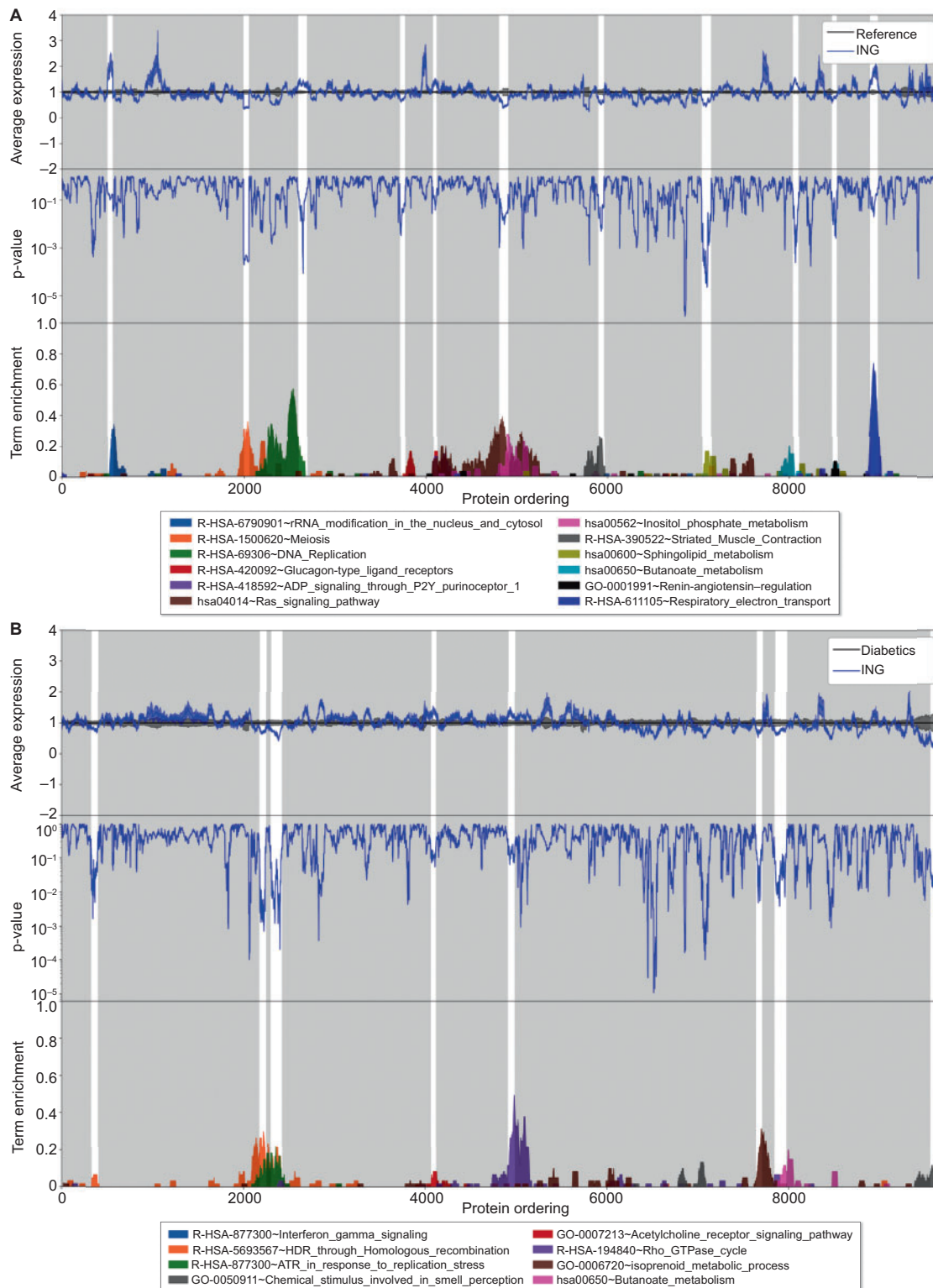
FIGURE 6: A transcriptogram network analysis was performed for two comparisons. (**A**) Idiopathic nodular samples (ING) and REF samples were compared revealing enrichment of the pathways listed (all P < 0.05 after multiple testing correction). (**B**) Idiopathic nodular samples and diabetic nodular glomerulosclerosis samples (diabetics) were compared revealing enrichment of the pathways listed (all P < 0.05 after multiple testing correction). In each transcriptogram, genes are ordered on the *x*-axis according to known protein–protein interactions. The top panel coveys the regional expression difference and direction of effect of ING (blue line) as compared with the normalized expression for the REF or diabetic expression (black line). In the second panel, regional corrected significance is provided. In the bottom panel, selected significant pathways are plotted with their degree of enrichment.
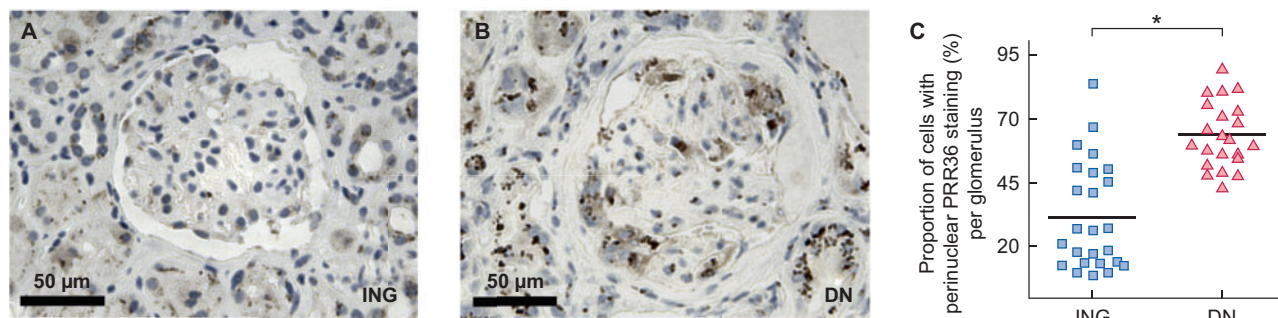
M.T. Eadon *et al.*

FIGURE 7: Immunohistochemistry of PRR36 in (**A**) idiopathic nodular samples ($n = 5$) and (**B**) nodular DN samples ($n = 5$). (**C**) The proportion of cells with perinuclear expression per glomerulus. In idiopathic nodular samples, 31.7% of cells had a perinuclear reaction compared with 63.1% of diabetic samples (P $= 0.01$). Each dot represents the proportion of cells with expression in a glomerulus. Between four and six nonobsolescent glomeruli were counted per section.

2. Herzenberg AM, Holden JK, Singh S *et al.* Idiopathic nodular glomerulosclerosis. *Am J Kidney Dis* 1999; 34: 560–564
3. Markowitz GS, Lin J, Valeri AM *et al.* Idiopathic nodular glomerulosclerosis is a distinct clinicopathologic entity linked to hypertension and smoking. *Hum Pathol* 2002; 33: 826–835
4. Wu J, Yu S, Tejwani V *et al.* Idiopathic nodular glomerulosclerosis in Chinese patients: a clinicopathologic study of 20 cases. *Clin Exp Nephrol* 2014; 18: 865–875
5. Li W, Verani RR. Idiopathic nodular glomerulosclerosis: a clinicopathologic study of 15 cases. *Hum Pathol* 2008; 39: 1771–1776
6. Hamrahian M, Mollaee M, Anand M *et al.* Impaired glucose metabolism - A potential risk factor for idiopathic nodular glomerulosclerosis: a single center study. *Med Hypotheses* 2018; 121: 95–98
7. Salvatore SP, Troxell ML, Hecox D *et al.* Smoking-related glomerulopathy: expanding the morphologic spectrum. *Am J Nephrol* 2015; 41: 66–72
8. Nakamura N, Taguchi K, Miyazono Y *et al.* AGEs-RAGE overexpression in a patient with smoking-related idiopathic nodular glomerulosclerosis. *CEN Case Rep* 2018; 7: 48–54
9. Chandragiri S, Raju S, Mukku KK *et al.* Idiopathic nodular glomerulosclerosis: report of two cases and review of literature. *Indian J Nephrol* 2016; 26: 145–148
10. Alicic RZ, Rooney MT, Tuttle KR. Diabetic kidney disease: challenges, progress, and possibilities. *Clin J Am Soc Nephrol* 2017; 12: 2032–2045
11. Reidy K, Kang HM, Hostetter T *et al.* Molecular mechanisms of diabetic kidney disease. *J Clin Invest* 2014; 124: 2333–2340
12. Tervaert TW, Mooyaart AL, Amann K *et al.* Pathologic classification of diabetic nephropathy. *J Am Soc Nephrol* 2010; 21: 556–563
13. Eadon MT, Schwantes-An TH, Phillips CL *et al.* Kidney histopathology and prediction of kidney failure: a retrospective cohort study. *Am J Kidney Dis* 2020; 11: 350–360
14. Lusco MA, Fogo AB, Najafian B *et al.* AJKD atlas of renal pathology: idiopathic nodular sclerosis. *Am J Kidney Dis* 2016; 68: e19–e20
15. Stout LC, Kumar S, Whorton EB. Focal mesangiolysis and the pathogenesis of the Kimmelstiel-Wilson nodule. *Hum Pathol* 1993; 24: 77–89
16. Colvin RC. *Diagnostic Pathology: Kidney Diseases,* 3rd edn. Amsterdam, The Netherlands: Elsevier, 2019
17. Barwinska D, Ferkowicz MJ, Cheng YH *et al.* Application of laser microdissection to uncover regional transcriptomics in human kidney tissue. *J Vis Exp* 2020; 160: doi: 10.3791/61371
18. Amini P, Ettlin J, Opitz L *et al.* An optimised protocol for isolation of RNA from small sections of laser-capture microdissected FFPE tissue amenable for next-generation sequencing. *BMC Mol Biol* 2017; 18: 22
19. Zhao S, Fung-Leung WP, Bittner A *et al.* Comparison of RNA-Seq and microarray in transcriptome profiling of activated T cells. *PLoS One* 2014; 9: e78644
20. Li S, Tighe SW, Nicolet CM *et al.* Multi-platform assessment of transcriptome profiling using RNA-seq in the ABRF next-generation sequencing study. *Nat Biotechnol* 2014; 32: 915–925
21. Dobin A, Davis CA, Schlesinger F *et al.* STAR: ultrafast universal RNA-seq aligner. *Bioinformatics* 2013; 29: 15–21
22. Liao Y, Smyth GK, Shi W. featureCounts: an efficient general purpose program for assigning sequence reads to genomic features. *Bioinformatics* 2014; 30: 923–930
23. Robinson MD, McCarthy DJ, Smyth GK. edge R: a Bioconductor package for differential expression analysis of digital gene expression data. *Bioinformatics* 2010; 26: 139–140
24. Robinson MD, Smyth GK. Small-sample estimation of negative binomial dispersion, with applications to SAGE data. *Biostatistics* 2007; 9: 321–332
25. Fabregat A, Jupe S, Matthews L *et al.* The reactome pathway knowledgebase. *Nucleic Acids Res* 2018; 46: D649–D655
26. Boyle EI, Weng S, Gollub J *et al.* GO: term finder–open source software for accessing gene ontology information and finding significantly enriched gene ontology terms associated with a list of genes. *Bioinformatics* 2004; 20: 3710–3715
27. Yu G, He QY. ReactomePA: an R/Bioconductor package for reactome pathway analysis and visualization. *Mol Biosyst* 2016; 12: 477–479
28. Yu G, Wang LG, Han Y *et al.* clusterProfiler: an R package for comparing biological themes among gene clusters. *OMICS* 2012; 16: 284–287
29. de Almeida RM, Clendenon SG, Richards WG *et al.* Transcriptome analysis reveals manifold mechanisms of cyst development in ADPKD. *Hum Genomics* 2016; 10: 37
30. O'Leary NA, Wright MW, Brister JR *et al.* Reference sequence (RefSeq) database at NCBI: current status, taxonomic expansion, and functional annotation. *Nucleic Acids Res* 2016; 44: D733–D745
31. Song J, Liu YD, Su J *et al.* Systematic analysis of alternative splicing signature unveils prognostic predictor for kidney renal clear cell carcinoma. *J Cell Physiol* 2019; 234: 22753–22764
32. Chen L, Wu H, Pochynyuk OM *et al.* Af17 deficiency increases sodium excretion and decreases blood pressure. *J Am Soc Nephrol* 2011; 22: 1076–1086
33. Stout LC, Whorton EB. Pathogenesis of extra efferent vessel development in diabetic glomeruli. *Hum Pathol* 2007; 38: 1167–1177
34. Osterby R, Asplund J, Bangstad HJ *et al.* Neovascularization at the vascular pole region in diabetic glomerulopathy. *Nephrol Dial Transplant* 1999; 14: 348–352
35. Rao J, Ashraf S, Tan W *et al.* Advillin acts upstream of phospholipase C 1 in steroid-resistant nephrotic syndrome. *J Clin Invest* 2017; 127: 4257–4269
36. Boyer O, Benoit G, Gribouval O *et al.* Mutational analysis of the PLCE1 gene in steroid resistant nephrotic syndrome. *J Med Genet* 2010; 47: 445–452

37. Hinkes B, Wiggins RC, Gbadegesin R *et al.* Positional cloning uncovers mutations in PLCE1 responsible for a nephrotic syndrome variant that may be reversible. *Nat Genet* 2006; 38: 1397–1405

38. Woroniecka KI, Park AS, Mohtat D *et al.* Transcriptome analysis of human diabetic kidney disease. *Diabetes* 2011; 60: 2354–2369

39. Altiparmak MR, Pamuk ON, Pamuk GE *et al.* Diffuse diabetic glomerulosclerosis in a patient with impaired glucose tolerance: report on a patient who later develops diabetes mellitus. *Neth J Med* 2002; 60: 260–262

40. Souraty P, Nast CC, Mehrotra R *et al.* Nodular glomerulosclerosis in a patient with metabolic syndrome without diabetes. *Nat Rev Nephrol* 2008; 4: 639–642

41. Gonzalez A, Krieg R, Massey HD *et al.* Sodium butyrate ameliorates insulin resistance and renal failure in CKD rats by modulating intestinal permeability and mucin expression. *Nephrol Dial Transplant* 2019; 34: 783–794

42. Matsumoto N, Riley S, Fraser D *et al.* Butyrate modulates TGF-beta1 generation and function: potential renal benefit for Acacia(sen) SUPERGUM (gum arabic)? *Kidney Int* 2006; 69: 257–265

M.T. Eadon *et al.*